ELSEVIER

Thermochimica Acta 319 (1998) 33–42

thermochimica acta

Conductrometric, density and thermal measurements of the $M_2S_2O_7$ (M=Na, K, Rb, Cs) salts

G. Hatem[a,*], F. Abdoun[a], M. Gaune-Escard[a], K.M. Eriksen[b], R. Fehrmann[b]

[a] *Institut Universitaire des Systémes Thermiques Industriels, Associé au CNRS-UMR 6595, 5, rue Enrico Fermi, 13453 Marseille cedex 13, France*

[b] *Department of Chemistry, Technical University of Denmark, DK-2800 Lyngby, Denmark*

Received 28 July 1997; accepted 1 May 1998

Abstract

Physico-chemical properties, such as densities, conductivities, enthalpies of phase transitions and melting points, have been measured and summarised for the alkali pyrosulphates $Na_2S_2O_7$, $K_2S_2O_7$, $Rb_2S_2O_7$, $Cs_2S_2O_7$. The densities of the molten pyrosulphates could be expressed by the linear expression $\rho=A+B(T-T_m)$ where T_m is the middle temperature of the temperature range measured, i.e. from the melting point and up to 550°C at the maximum.

The specific conductivities of the molten pyrosulphates have been expressed by the equation $\rho=A+B(T-T_m)+C(T-T_m)^2+D(T-T_m)^3$ in the temperature range from the melting point and up to 500°C at the maximum. From these measurements also the activation energy for the equivalent conductivity of the alkali cations in the melts could be calculated and compared to the analogous alkalisulphates.

By calorimetric investigations of the alkali pyrosulphates the temperatures of fusion, the enthalpies and entropies of fusion and possible solid–solid transitions together with the molar heat capacities of the solid and liquid pyrosulphates at 300–800 K, have been obtained and discussed in relation to the conductrometric measurements and the few related previous investigations.

Keywords: Alkalipyrosulphates; Conductivity; Density; Heat capacities; Heats of transitions; Melting points

1. Introduction

The ternary $M_2S_2O_7$–$MHSO_4$–V_2O_5 (M=Na, K, Rb, Cs) molten salt system plays a major role as catalyst for the oxidation of SO_2 to SO_3 by O_2 for the manufacture of sulphuric acid or in the purification of flue gases emitted, for example, by power plants [1–10].

In these catalytic processes, the active component is vanadium oxo-sulphato complexes, such as $VO_2SO_4^-$, $(VO)_2O(SO_4)_4^{4-}$, $VO_2(SO_4)_2^{3-}$ $\cdots$ and the polymeric complexes $(VO_2SO_4)_n^{n-}$ and $(VO_2(SO_4)_2)_n^{3n-}$, that seem to be formed depending on the mole fraction $x(V_2O_5)$ of the mixtures [1,4,8–10].

In order to identify these complexes several investigations have been undertaken by means of spectroscopic, density, thermal and electrochemical methods.

Analysis of the results is possible if the data can be compared to those obtained from the pure components.

---

*Corresponding author. Tel.: +33 491 106888; fax: +33 491 106969.

PII S0040-6031(98)00396-7

This paper is devoted to measurements of the electrical conductivity, density, temperature and enthalpy changes by solid–solid or solid–liquid transitions and the heat capacity of the liquid and solid, alkali-pyrosulphates – the solvents for the catalytically active vanadium species.

Lithium is not a promoter for the catalysis and in addition $Li_2S_2O_7$ starts to decompose well below the melting point [13,14]. For these reasons $Li_2S_2O_7$ is not dealt with in the present work.

2. Experimental

2.1. Chemicals

Pure and dry $M_2S_2O_7$ was obtained by thermal decomposition of $M_2S_2O_8$ (Merck–Pro Analysi) for Na and K or synthesized in the laboratory for Rb and Cs [3,11].

All handling of chemicals took place in a nitrogen or an argon filled glovebox with a measured water content of ca. 5 ppm. Prior to use the salts were kept in sealed ampoules and cut open in the glovebox only.

2.2. Density

The densities were measured using Archimedean's principle by measuring the apparent weight of a spherical platinum bob dipped into a quartz crucible containing the melt as described earlier [12].

The density was obtained from the expression: $\rho = \Delta m/V_t(\mathrm{g\,cm^{-3}})$, where Δm is the weight difference of the bob in argon and the melt and V_t the volume of the bob at the temperature t. The volume of the bob, at the measuring temperature (in °C), was obtained from the equation:

$$V_t = V_{0^\circ\mathrm{C}}(1+0.2554\times10^{-4}t+0.0104\times10^{-6}t^2)$$

After each series of measurements the weight loss did not exceed 1%. This loss is possibly due to decomposition of $M_2S_2O_7$ into SO_3 and M_2SO_4. Due to this decomposition the maximum experimental temperature did not exceed 80 K above the melting point.

The accuracy of the temperature of the melt during the experiments was within ±2 K because of the vertical temperature gradient along the crucible. The relative error of the mass determination was ca. ±0.05%. By taking into account the errors of the mass and temperature, the estimated error of the density was 0.2%.

2.3. Conductivity

The borosilicate glass cell, with gold electrodes, used for measuring the electrical conductivity, has been described in detail previously [12]. The cell was filled in the dry box, sealed and placed in the measuring furnace regulated to within ±0.1 K. The resistance of the cell was measured when it was constant. The temperature was lowered in steps of 2–10 K, and subcooling was generally observed, indicated by a sudden jump in the resistance to a much higher value when crystallization occurred. The temperature was measured by a calibrated Pt(100) platinum resistance thermometre placed directly at the capillary tube of the conductivity cell. The conductivity was measured by a Radiometer CDM-83 conductivity meter.

The cell constants were determined at room temperature in a thermostat using a 0.1 Demal KCl standard solution as described in Ref. [15].

2.4. Thermal investigations

The temperatures of the phase transitions, solid–solid or solid–liquid, and the heat involved in these transitions, have been measured with a Calvet microcalorimeter. This apparatus has been described previously [1,16]. The borosilicate glass cells containing the alkali-pyrosulphates were filled in the glovebox and sealed under vacuum. The large number of thermocouples in the two calorimetric cells and the very low heating rate (3–10 K $\mathrm{h^{-1}}$), controlled by a linear temperature programmer resulted in high quality thermograms, with a very well-defined base line and separation of thermal effects occurring at very close temperatures. The calorimetre temperature is controlled by a calibrated Pt(100) platinum resistance thermometer in order to obtain a linear variation of the temperature vs. time. The experimental temperature is measured by a Pt/Pt-10%Rh thermocouple located near the cell containing the salt. It was checked in a separate experiment towards the melting point of lead. The heat, Q, involved during the phase transition is linked to the area, S, of the thermogram by the linear relation: $Q=KS$, where K is the calorimeter constant. This constant is determined in a separate experiment with the same heating rate on a sample of lead. Temperature and enthalpy of melting of lead are given in Ref. [17] as $T_{\text{fus}}=600$ K and $\Delta_{\text{fus}}H=4.81$ kJ mol^{-1}.

Heat capacity measurements were carried out with a Setaram DSC 121 differential scanning calorimeter. The apparatus and the measuring procedure have been described in detail previously [18].

The measuring method used was the so-called 'step-method', developed by Setaram [19]: small heating steps are followed by isothermal delays, when thermal equilibrium of the sample is achieved. Two correlated experiments should be carried out with this method to determine the heat capacity of the sample. The first one, with two empty cells (containers) of the same mass and the second with the same cells, but one of them containing the sample. Heat flux as a function of time and temperature is recorded for both runs. The difference of heat flux in both runs is proportional to the amount of heat necessary to increase the temperature of the sample by ΔT. Therefore, the value of the heat capacity of the sample is equal to: $c_p=QM/(\Delta Tm)$, where m is the mass of the sample and M the molar mass of the sample. The same conditions for both experiments (i.e. starting temperature, temperature increment and isothermal delay) are required. All necessary calculations are performed by the original Setaram program.

The apparatus was calibrated by Joule effect. Additionally, some test measurements with NBS Standard Reference material 720 α-Al_2O_3 have been carried out before the investigations.

Quartz cells of 7 mm in diametre and 15 mm of length were filled in the glovebox, sealed under vacuum and then placed in the calorimeter. Measurements were performed by heating steps of 5 K followed by 400 s isothermal delay. The heating rate was 2 K min^{-1}. All experiments were started at 300 K and performed up to 750–800 K.

3. Results and discussion

3.1. Density measurements

Table 1
Experimental densities of molten $Na_2S_2O_7$ and $Rb_2S_2O_7$

T/K	Density/(g cm^{-3})		T/K	Density/(g cm^{-3})	
	$Na_2S_2O_7$	$Rb_2S_2O_7$		$Na_2S_2O_7$	$Rb_2S_2O_7$
678	2.1725		725	2.1488	
680	2.1695		727	2.1454	
685	2.1695		732	2.14	
689	2.1654		733	2.1414	
689	2.1636		733		2.8107
694	2.1646		735		2.8025
700	2.1591		736		2.8064
702	2.1563		737		2.8003
703	2.1581		737		2.8043
706		2.8333	739	2.1317	
709		2.829	740		2.806
713		2.8226	743		2.7957
715	2.1505		745		2.7995
715		2.8224	745		2.7975
717	2.1511		747		2.7914
718		2.8182	750		2.7951
720	2.1534		752		2.7949
720		2.818	753		2.7868
722		2.8178	758		2.7883
722		2.8198	759		2.7862
723	2.1431		763		2.7798
723		2.8117	768		2.7793
723		2.8137	769		2.7832
723		2.8177	772		2.7809
724		2.8136	790		2.7512
725	2.1489				

The experimental densities and temperatures of the molten $Na_2S_2O_7$ and $Rb_2S_2O_7$ salts are given in Table 1. The investigated temperature range was 675–740 and 705–795 K for $Na_2S_2O_7$ and $Rb_2S_2O_7$, respectively.

No density value of these salts have been found in the literature.

In Table 2, the measured densities are expressed by the linear equation: $\rho=A+B(T-T_m)$, where ρ is the density in g cm^{-3}, T the temperature in K and T_m the

Table 2
Linear density equations, $\rho=A+B(T-T_m)$ and molar volume at Tm of molten alkali pyrosulphates

Compound	A/ (g cm^{-3})	1000×B/ (g cm^{-3} K)	Tm/ K	SE/ (g cm^{-3})	V_m/ cm^3
$Na_2S_2O_7$	2.154(6)	−0.568(32)	710	0.002	102.82
$K_2S_2O_7$	2.080(1)	−0.650(27)	723	0.001	121.40
$Rb_2S_2O_7$	2.801(13)	−0.845(29)	740	0.0003	122.42
$Cs_2S_2O_7$	2.9222(15)	−0.907(28)	773	0.0001	144.51

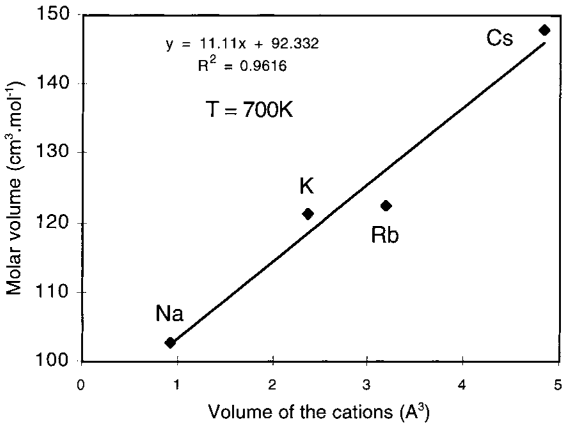

Fig. 1. Molar volume of molten alkali pyrosulphates vs. the volume of the alkali cations.

middle temperature of the temperature range. As described previously [20], this expression gives a more satisfactory representation of the measured data than the usually employed equation: $\rho=A+BT$.

Densities of $K_2S_2O_7$ and $Cs_2S_2O_7$ have earlier been measured [1,12], but for comparison we present the coefficients A and B for all of the investigated pyrosulphates, in Table 2. In this table, the values for the coefficients of the linear analytical expressions and the SE for each molten salt are given.

Table 2 also lists the values of the molar volume of the alkali pyrosulphates at 700 K calculated from the linear expressions. In Fig. 1, these molar volumes are plotted against the volume of the alkali ions and as it can be seen in this figure, a linear dependence might be assumed.

3.2. Conductivity measurements

The conductivity has been measured in the 639–700 K range for $Na_2S_2O_7$ and 670–753 K for $Rb_2S_2O_7$ due to the different melting points of the alkali pyrosulphates.

The experiments were performed by cooling or by heating in steps of 2–10 K; close to the phase transitions the steps were usually 2 K.

We have fitted the experimental data for the liquid range to polynomials of the type [20]: $\kappa = A + B(T-T_m) + C(T-T_m)^2 + D(T-T_m)^3$, where κ is the conductivity in Ω^{-1} cm^{-1}, T the temperature in Kelvin and T_m the middle temperature of the temperature range.

Table 3
Specific conductivity, κ (Ω^{-1} cm^{-1}), for alkali pyrosulphates

T/K	$Na_2S_2O_7$	$Rb_2S_2O_7$	T/K	$Na_2S_2O_7$	$Rb_2S_2O_7$
639.6	0.00049		680.8	0.40716	
644.2	0.00061		681		0.012
649.4	0.00081		681.2		0.01119
649.4	0.00079		683	0.4135	
650.5	0.00143		683.6	0.41857	
654	0.0012		683.7	0.41604	
654.2	0.00119		685.3	0.41875	
656.2	0.34247		685.8	0.42238	
657.1	0.0018		687.5	1.45444	
659.5	0.34881		689.9	1.44958	
659.6	0.34678		691.3		0.18889
660.1	0.00355		691.4		0.01771
660.3	0.00541		691.7	1.44564	
662.8	0.00718		693.4	1.442252	
663.1	0.00608		695.9	1.436905	
664.1	0.36276		696.3		0.19674
664.7	0.00929		697.8	1.433116	
666.2	0.00846		698.5		0.02006
666.6	0.01088		701.1		0.02307
669	0.37671		701.5		0.20522
669.3	0.01175		706.3		0.02926
669.6	0.37513		711.4		0.2209
670.5	0.01762		711.4		0.03646
671.2		0.00884	716.5		0.05194
672.5	0.02484		721.2		0.08098
672.6	0.02258		721.5		0.2385
673.6	0.3894		724		0.23977
675.5	0.04503		725.9		0.2455
676.4	0.0099		730.9		0.25228
676.4	0.06936		731		0.25228
678.2	0.18495		736.3		0.265
678.8	0.17123		741.8		0.26924
679.4	0.40589		746.6		0.27984
679.7	0.40567		749.2		0.28408
680.4	0.40349		752.6		0.29044

All the experimental values are given in Table 3 and the coefficients of the polynomial equations are given in Table 4, together with those previously obtained for $K_2S_2O_7$ [12] and $Cs_2S_2O_7$ [1]. Empirically it has been found that κ is exponentially related to the temperature [21–23] as $\kappa=A(\kappa)e^{-E(\kappa)/RT}$, where $A(\kappa)$ is a constant, $E(\kappa)$ is the energy necessary to promote the ionic migration and R and T have their usual meanings. $E(\kappa)$ is, in general, dependent on the temperature and its value changes drastically by going from the liquid to the solid phase. Therefore, a plot of $\ln(\kappa)$ vs. the inverse temperature, $1/T$, shows a break at the phase-transition temperature [21].

Table 4
Coefficients for the emperical equations [a] for the specific conductivity of the alkali pyrosulphates

	$A/(\Omega^{-1}\,\mathrm{cm}^{-1})$	$10^3B/(\Omega^{-1}\,\mathrm{cm}^{-1}\mathrm{K}^{-1})$	$10^6C/(\Omega^{-1}\,\mathrm{cm}^{-1}\mathrm{K}^{-2})$	$10^8D/(\Omega^{-1}\,\mathrm{cm}^{-1}\mathrm{K}^{-3})$	$\mathrm{SD}/(\Omega^{-1}\,\mathrm{cm}^{-1})$
Na	0.435533	2.8628	−16.149	0	0.0033
K	0.296343	1.9935	1.831	2.555	0.0011
Rb	0.261654	1.7577	2.695	−31.869	0.0031
Cs	0.21517	1.3859	3.732	−5.826	0.0004

[a] $\kappa = A+B(T-T_m)+C(T-T_m)^2+D(T-T_m)^3$, where T_m is equal to 688 K for $Na_2S_2O_7$ and 723 K for all the other salts.

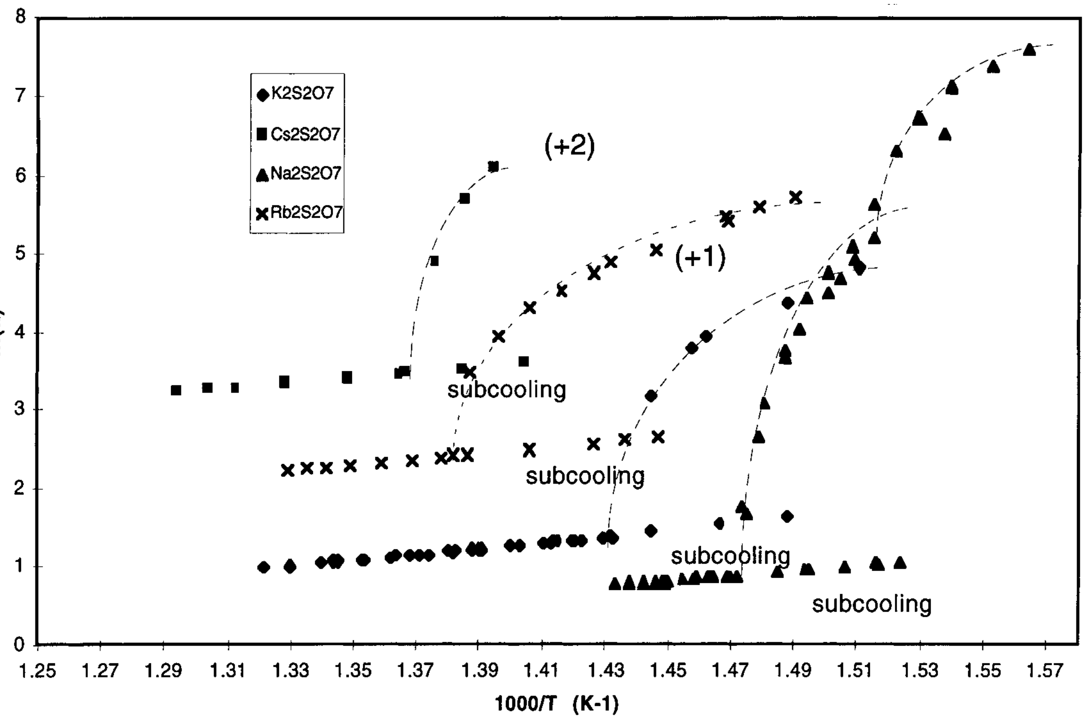

Fig. 2. Electrical conductivities of the alkali pyrosulphates: $-\ln(\kappa)$ vs. $1/T$. For clarity, the data for Rb and Cs are offset on the ordinate by the specified values.

In Fig. 2, we have plotted $-\ln(\kappa)$ vs. $1/T$. From the observed breaks on the conductivity curves the melting points of the pyrosulphates have been obtained and the values will be discussed below. A pronounced tendency to subcooling of the molten pyrosulphates is also observed.

On the basis of the measured conductivities, the densities from the polynomials and the assumption that the alkali ions M^+ are carrying all the current, the equivalent conductivity of these ions, ΛM^+, can be calculated by applying the equation: $\Lambda M^+ = \kappa V^M/2 = Ae^{-E/RT}$, where V^M is the molar volume of the melt. This has been done for each alkali pyrosulphate and the parameters A and E are given in Table 5, together with values for the alkali sulphates deduced from Ref. [24]. Due to the size of the anions, the activation energy is higher for the pyrosulphates as compared to the corresponding sulphates.

Fig. 3 shows the activation energy for the series of these salts vs. the radius of the cations and for the alkali fluorides, chlorides, bromides, iodides and nitrates found in Ref. [24]. From these curves, it is observed that the activation energy increases from Na to Cs but for cesium sulphate and pyrosulphate, the

Table 5
Activation energy parameters[a] for alkali sulphates and pyrosulphates

	Pyrosulphates		Sulphates [24]	
	A/ (Ω^{-1} cm^2 mol^{-1})	E/ kJ	A/ (Ω^{-1} cm^2 mol^{-1})	E/ kJ
Na	2884	27.90	550	18.86
K	3240	31.20	815	19.76
Rd	3089	30.48	472	20.74
Cs	1703	28.04	387	18.94

[a] $\Lambda M^+ = Ae^{-E/RT}$.

activation energy is lower than excepted from this tendency. In spite of the size of the cesium ion, it seems that the ionic migration is higher than for the smaller ones. This effect is probably due to a change in the liquid structure whereby, for example, the weaker interaction between the large Cs^+ cation and the sulphate or pyrosulphate anions makes possible a larger anion migration and contribution to the conductivity of the melt.

3.3. Thermal analysis

3.3.1. $Na_2S_2O_7$

In order to determine the temperatures and enthalpies of transitions, several thermal cycles (heating and cooling) have been performed in the 300–720 K range, using either the differential scanning calorimetre or the Calvet calorimeter.

In Ref. [25], indication has been given, from heat capacity measurements, about a possible polymorphic transformation just below the melting point. Indeed, ca. 630 K, the shape of our thermograms, obtained by differential enthalpic analysis, seem to indicate either

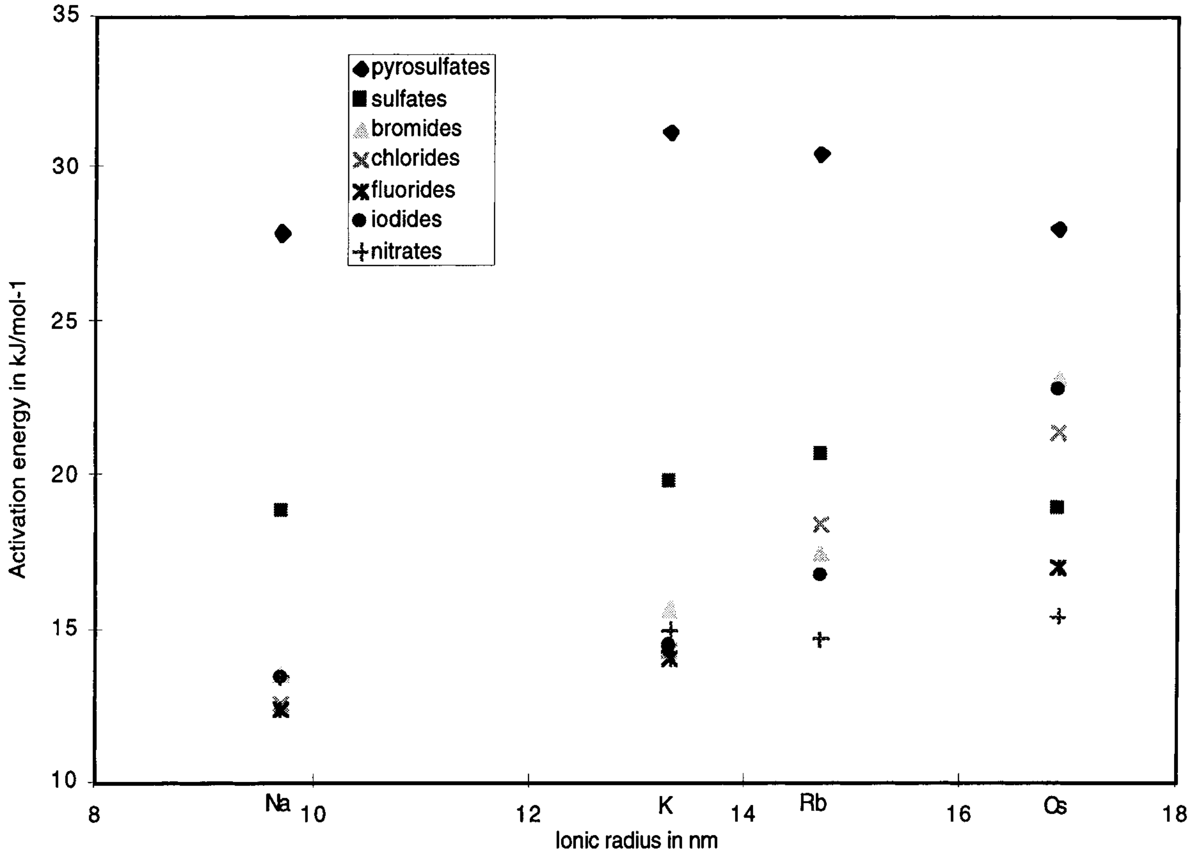

Fig. 3. Activation energy for ionic migration vs. the radius of the alkali cations.

a solid–solid transition just before the melting point or a premelting effect. We have tried to separate these two possible thermal effects obtained, by decreasing the heating rate from 10 to 1 K h^{-1}. No solid–solid transition has been clearly evidenced in this temperature range and, as for Li_2SO_4 [26,27], this behaviour is probably due to a premelting effect. From the plot of $-\ln\kappa$, vs. $1/T$, Fig. 2, the break point at 660 K could indeed be due to either a solid–solid transition or a premelting effect.

Further investigations of the structure vs. temperature by NMR, are in progress.

Ten measurements, using 10 samples, have been performed to obtain the temperature and enthalpy of melting. The average of the values obtained is: $T_{\mathrm{fus}} = 674 \pm 5$ K; $\Delta_{\mathrm{fus}}H = 41.7 \pm 2.3$ kJ mol^{-1}.

A small solid–solid transition has been found at 451 K, $\Delta_{\mathrm{trans}}H$=1.78 kJ mol^{-1}. Due to the premelting effect, the accuracy, particularly for the temperature of melting is poor.

From our conductometric measurements we obtained by plotting $-\ln\kappa$ vs. $1/T$ (Fig. 2), a temperature of fusion of 679 K. The deviation of 5 K, from the DTA value is probably due to the fact that this latter value corresponds to the beginning of melting (onset temperature), whereas the temperature obtained by conductometry corresponds to the end of the melting process and can be compared with the temperature obtained at the top of the thermogram (679±1 K).

The values of the melting point found in the literature are not very scattered: 676 K [28], 674 K [29], 669 K [30], 675 K [14], 673 K [31], 663 K [32].

For the heat of fusion, we have only found one value in the literature, namely 40.8±0.4 KJ mol^{-1} [25], in good agreement with our value.

The heat capacity has been measured in the 300–720 K range. The experimental data are given in Table 6 and, for the solid state in the 300–600 K range, fitted by the linear equation, C_p=A+BT.

From 600 K to the melting point, deviation of the heat capacity from this linear dependency was observed (Fig. 4) and could be allocated to the premelting effect.

As is often observed for molten salts, we have not detected an important variation of the heat capacity and an average of the data has been calculated. All parameters are given in Table 7.

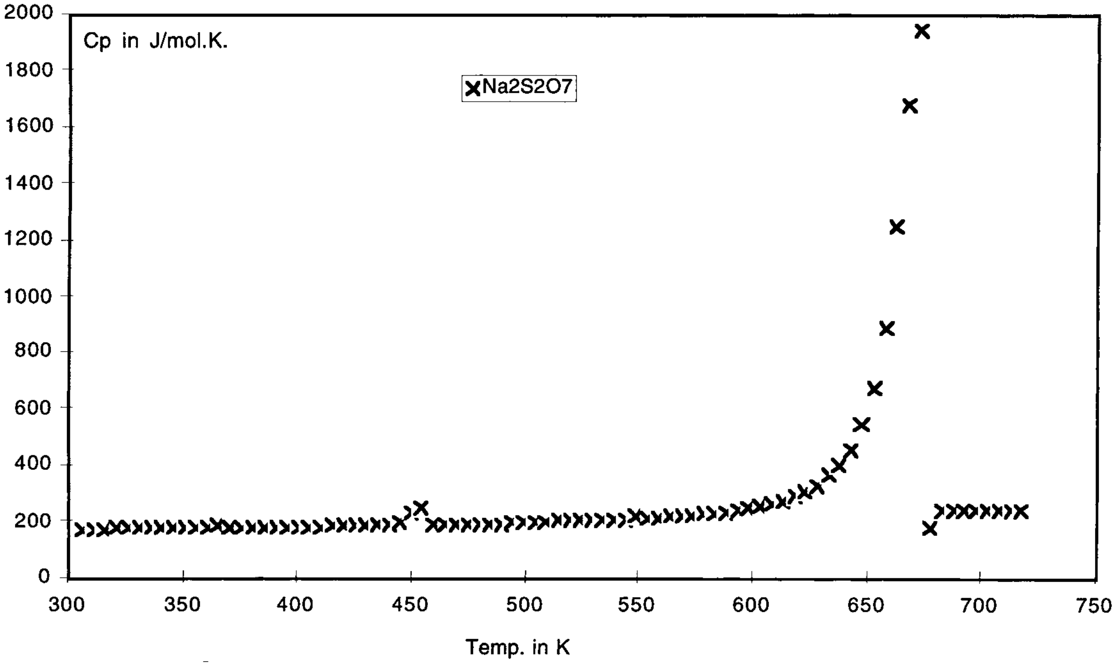

Fig. 4. Molar heat capacity of $Na_2S_2O_7$.

Table 6
Molar heat capacities for alkali pyrosulphates $M_2S_2O_7$ (M=Na, K, Rb, Cs)

T/K	C_p/(J mol^{-1} K^{-1})				*T*/K	C_p/(J mol^{-1} K^{-1})			
	Na	K	Rb	Cs		Na	K	Rd	Cs
306	172.5	190.7	209.3	209.5	534	206.7	227.1	236.0	255.4
311	173.6	188.9	214.8	210.8	539	208.1	223.8	236.0	258.5
316	174.5	185.9	216.2	212.6	544	209.6	225.1	238.1	271.8
321	176.1	192.0	216.9	213.9	549	223.4	226.8	236.7	296.5
326	176.5	194.8	220.0	209.5	554	213.6	229.6	236.3	236.0
331	177.4	195.3	226.3	213.0	559	215.6	232.4	236.7	267.4
336	177.0	196.8	231.1	214.3	564	219.6	231.4	238.8	264.3
341	178.8	197.1	230.8	212.6	569	220.5	236.0	238.8	268.7
346	178.1	195.8	232.9	210.8	574	223.2	239.3	239.8	270.0
351	177.2	194.3	233.2	226.7	579	227.8	242.3	240.1	270.9
356	178.3	193.3	222.5	228.5	584	232.3	242.1	241.2	271.8
361	180.5	196.6	226.6	230.2	589	235.8	245.7	239.5	274.4
366	185.6	201.9	219.7	228.0	593				279.3
370				225.8	594	240.9	209.3	239.1	
371	177.9	204.2	220.4		598				276.2
375				231.1	599	248.7	2807.9	239.5	
376	178.5	190.5	220.0		603				284.6
380				234.2	604	256.3	184.1	241.9	
381	178.3	195.6	233.2		608	265.6	261.9	241.5	307.1
385	179.4	213.6		235.1	613	275.3	261.2	239.8	266.0
386			239.8		618	290.4	261.2	239.5	278.4
390	179.9	205.7		232.5	623	307.3	262.9	239.5	278.4
391			236.0		628	330.6	264.7	242.2	286.4
395	181.4	207.3	234.2	227.1	633	364.2	258.6	243.3	283.3
400	182.1	212.6	239.5	230.2	638	404.8	257.6	242.9	292.1
405	182.8	212.1	236.7	238.6	643	459.7	254.8	242.9	297.4
410	182.5	213.9	236.7	242.2	648	541.8	256.6	241.5	304.9
415	183.2	210.8	237.7	240.8	653	673.3	254.6	243.6	316.0
420	186.1	209.3	238.4	247.5	658	892.4	255.6	242.2	321.7
425	184.3	210.0	236.0	244.8	663	1248.4	260.7	244.0	337.2
430	188.1	210.0	237.0	263.4	668	1675.2	269.3	244.0	354.4
435	191.2	210.0	236.0	368.1	673	1943.6	310.8	241.9	365.5
440	191.4	210.3	233.6	249.7	678	178.3	402.6	245.4	404.8
445	197.4	210.6	232.9	233.8	683	245.8	702.4	242.9	443.2
450	233.6	212.6	235.3	244.4	688	243.6	1722.9	244.7	504.7
455	253.1	212.6	236.0	250.1	693	244.3	942.9	244.3	591.7
460	193.4	210.8	237.0	244.8	698	243.8	268.8	249.5	728.7
465	193.0	216.2	236.7	235.1	703	244.3	264.2	261.3	890.5
470	192.5	217.2	237.0	242.6	708	244.7	269.0	319.6	852.0
475	194.1	217.7		245.3	712				325.3
480	193.4	217.9		246.6	713	245.6	265.2	620.8	
484				245.7	717	246.5	266.0		299.2
485	195.2	218.4			718			2937.3	
489				249.2	722			26.4	297.4
490	197.0	221.2			727			274.2	291.2
494	199.4	219.5		245.3	732			274.2	297.0
499	200.1	226.6	239.1	247.0	737			272.8	293.4
504	202.1	237.3	236.7	255.0	742			272.8	293.4
509	203.8	227.1	231.8	244.4	747			270.7	290.3
514	207.2	226.8	235.3	249.2	752			272.1	289.0
519			233.9	250.1	757			269.3	289.9
520	204.5	227.3			762				289.9
524	205.2	227.3	233.2	253.7	767				284.6
529	204.7	227.3	236.3	255.0					

Table 7
Coefficients of the linear equations for the heat capacity of alkali pyrosulphates

Compound	Solid phase			Solid phase	Liquid phase
	$C_p=A+BT$			C_p/(J mol^{-1} K^{-1})	C_p/(J mol^{-1} K^{-1})
	A/(J mol^{-1} K^{-1})		B/(J mol^{-1})		
		$300<T/K<590$			$680<T/K<720$
$Na_2S_2O_7$	110.2±3.6		0.187±0.008		244.8±1.0
		$300<T/K<590$		$591<T/K<692$	$680<T/K<717$
$K_2S_2O_7$	183±1		0.177±0.007	260±4	267±2
		$300<T/K<700$			$724<T/K<757$
$Rb_2S_2O_7$	207.4±1.2		0.057±0.04		272.2±1.8
		$300<T/K<710$			$717<T/K<777$
$Cs_2S_2O_7$	147.5±1.9		0.212±0.010		222.3±4.3

3.3.2. $K_2S_2O_7$

All thermal data were published earlier [7]. Two solid–solid transitions appear at T=473 K and T=591 K; $\Delta_{trans}H$ (591 K)=21.8 kJ mol^{-1}. Temperature and enthalpy of melting are T_{fus}=692 K and $\Delta_{fus}H$=21.2 kJ mol^{-1}. The melting point deduced from our conductometric measurements, Fig. 2, is in good agreement with the DTA value.

The experimental values of the heat capacity are shown in Table 6 and the parameters are used to fit these data in Table 7.

3.3.3. $Rb_2S_2O_7$

The differential enthalpic analysis has been carried out by using a DSC 121 calorimeter. The heating rate was 5 K min^{-1}. Three cycles of heating and cooling were done in the 300–770 K range. A small solid–solid transition appeared at 495 K.

The sample fused at T_{fus}=708±2 K and the heat associated was $\Delta_{fus}H$=17.8±0.5 kJ mol^{-1}. A premelting effect was observed 50 K below the melting point but it could not be separated from the heat of fusion. From the conductivity measurements, we deduced the temperature of melting (Fig. 2) to be T_{fus}=723 K. As for the sodium pyrosulphate, this value is in good agreement with the temperature read at the top of the DEA thermogram (721 K) and the deviation between the values obtained by the two methods is allocated to the premelting effect.

The literature is poor about data for the melting parameters, we found only T_{fus}=674 K [14], far from our value. However, in that work, the $Rb_2S_2O_7$ was synthesized from sulphuric acid by heating the obtained hydrogen sulphate, a doubtful method of preparation of the pure pyrosulphate [33].

Heat capacities were measured in the 300–770 K range. The experimental data are shown in Table 6. All parameters deduced to fit these values are given in Table 7.

3.3.4. $Cs_2S_2O_7$

The thermal data have been published earlier [11], except those related to heat capacities and heat of melting which are reported here.

Two low-temperature solid–solid transitions were found at 438 K and 565 K, respectively. The temperature of melting is 728 K (735 K at the top of the thermogram), it compares well to the value of 734 K found from the conductivity measurements (Fig. 2).

The heat of melting has been determined by DEA to be $\Delta_{fus}H$=19.5 kJ mol^{-1}. Heat capacities were measured in the 300–770 K range. All values are given in Tables 6 and 7.

From the temperature and enthalpy of melting, we can calculate the entropy of melting of these alkali pyrosulphates. These values are given, together with the temperature and enthalpy of melting, in Table 8. We can conclude from this table, that the entropy of melting is rather constant, except for sodium pyrosulphate where the entropy is higher than for the other salts. However, as indicated above, for potassium pyrosulphate we have evidenced a solid–solid transition ($\beta\rightarrow\alpha$) at 591 K well below the melting point. If we add the entropy of this transition (36.9 J mol^{-1} K^{-1}) to the entropy of melting

Table 8
Temperatures, enthalpies and entropies of melting of alkali pyrosulphates

Compound	T_{fus}/K	T_{fus} (cond.)/K	$\Delta_{fus}H$/ (J mol^{-1})	$\Delta_{fus}S$/ (J mol^{-1} K^{-1})
$Na_2S_2O_7$	674	675	41700	62
$K_2S_2O_7$	692	692	21200	31
$Rb_2S_2O_7$	708	723	17800	25
$Cs_2S_2O_7$	728	734	19500	27

(30.6 J mol^{-1} K^{-1}) we obtain the value, 67.5 J mol^{-1} K^{-1}, similar to the entropy of melting of sodium pyrosulphate. Therefore, the structure of solid $Na_2S_2O_7$ is probably the same as of the solid phase β-$K_2S_2O_7$; the melting of $Na_2S_2O_7$ occurs directly from one phase, whereas for $K_2S_2O_7$ a solid transition is needed from a thermodynamic point of view. The low-temperature solid structures of $Rb_2S_2O_7$ and $Cs_2S_2O_7$ correspond probably to α-$K_2S_2O_7$, judged from their rather similar melting entropies and as for $Na_2S_2O_7$ the melting occurs directly from one phase. Only the X-ray structure of $K_2S_2O_7$ is reported in the literature. Attempts to grow suitable crystals of the other alkali pyrosulphates and determine their structures are in progress [34].

Acknowledgements

Danish Natural Science Research Council and the French National Centre of Science Research are thanked for financial support.

References

[1] G.E. Folkmann, G. Hatem, R. Fehrmann, M. Gaune-Escard, N.J. Bjerrum, Inorg. Chem. 32 (1993) 1559.

[2] K. Nielsen, R. Fehrmann, K.M. Eriksen, Inorg. Chem. 32 (1993) 4825.

[3] S. Boghosian, R. Fehrmann, N.J. Bjerrum, G.N. Papatheodorou, J. Catal. 119 (1989) 121.

[4] B.S. Bal'zhinimaev, A.A. Ivanov, O.B. Lapina, V.M. Mastikhin, K.I. Zamaraev, Faraday Discuss. Chem. Soc. 87 (1989) 133.

[5] K.M. Eriksen, D.A. Karydis, S. Boghosian, R. Fehrmann, J. Catal. 155 (1995) 32.

[6] N.H. Hansen, N.J. Bjerrum, J. Chem. Eng. Data 26 (1981) 13.

[7] K.M. Eriksen, R. Fehrmann, G. Hatem, M. Gaune-Escard, O.B. Lapina, V.M. Mastikhin, J. Phys. Chem. 100 (1996) 10771.

[8] D.A. Karydis, K.M. Eriksen, R. Fehrmann, S. Boghosian, J. Chem. Soc. Dalton Trans. (1994) 2151.

[9] S.G. Masters, A. Chrissanthopoulos, K.M. Eriksen, S. Boghosian, R. Fehrmann, J. Catal. 166 (1997) 16.

[10] O.B. Lapina, B.S. Balz,hinimeav, S. Boghosian, K.M. Eriksen, R. Fehrmann, Catal. Today, submitted.

[11] G.E. Folkmann, G. Hatem, R. Fehrmann, M. Gaune-Escard, N.J. Bjerrum, Inorg. Chem. 30 (1991) 4057.

[12] G. Hatem, R. Fehrmann, M. Gaune-Escard, N.J. Bjerrum, J. Phys. Chem. 91 (1987) 197.

[13] H. Flood, T. Förland, Acta Chem. Scand. 1 (1947) 781.

[14] V.I. Spitsyn, M.A. Meerov, J. Gen. Chem. (Engl. Transl.) 22 (1952) 963.

[15] G. Jones, B.C. Bradshaw, J. Am. Chem. Soc. 55 (1933) 1780.

[16] M. Gaune-Escard, in: R. Gale, D.G. Lovering (Eds), Molten Salt Techniques, Plenum Press, New York, 1991.

[17] O. Kubaschewski, E.L. Evans, Metallurgical Thermochemistry, 3rd edn., Pergamon Press, London, 1958.

[18] M. Gaune-Escard, A. Bogacz, L. Rycerz, W. Szczepaniak, J. Alloys Comp. 235 (1996) 176.

[19] SETARAM DSC 121 – Experimentations, B/03NEDSCF.

[20] H.A. Andreasen, N.J. Bjerrum, N.H. Hansen, J. Chem. Eng. Data 25 (1980) 236.

[21] Iu.K. Delimarskii, B.F. Markov (Eds.), Electrochemistry of Fused Salts, English Edition, The Sigma Press, Washington, DC, 1961.

[22] Heymann, Bloom, Nature 156 (1945) 479.

[23] Evstrop'ev, Bull. Acad. Sci. URSS 3 (1937) 359.

[24] G.J. Janz, F.W. Dampier, G.R. Lakshminarayanan, P.K. Lorenz, R.P.T.C. Tomkins, in Molten salts, vol. 1, NSRDS-NBS 15, 1968.

[25] P. Pascal, Nouveau traité de chimie minrale, vol. II, part 1, Masson (Ed.), Paris, 1963.

[26] G. Hatem, Thermochimica Acta 88 (1985) 433.

[27] A.R. Ubbelohde, in The molten state of matter, A Wiley-Interscience Publication, New York, 1978.

[28] Reznitski, Khomyakov, Vesnik. Moscow Univ., 14(2) (1959) 199.

[29] L. Cambi, G. Bozza, Ann. Chim. Applic. 13 (1923) 221.

[30] Wickert, Brennstoff-Wörme Kraft 11 (1959) 110.

[31] B.J. Meehan, S.A. Tariq, J.O. Hill, J. Thermal Anal. 12 (1977) 235.

[32] V.N. Gubareva, N.P. Bel'skaya, E.G. Pogodilova, V.M. Borisov, R.M. Stal, Zh. Prikl. Kim. 61(6) (1988) 1377.

[33] N.H. Hansen, R. Fehrmann, N.J. Bjerrum, Inorg. Chem. 21 (1982) 744.

[34] K. Nielsen, K.M. Eriksen, R. Fehrmann, work in progress.